ELSEVIER

Journal of Photochemistry and Photobiology A: Chemistry 145 (2001) 79–86

Journal of Photochemistry and Photobiology A:Chemistry

www.elsevier.com/locate/jphotochem

Separation of linkage isomers of trithiocyanato (4,4′,4″-tricarboxy-2,2′,6,2″-terpyridine)ruthenium(II) by pH-titration method and their application in nanocrystalline TiO_2-based solar cells

Md.K. Nazeeruddin*, M. Grätzel

Laboratory for Photonics and Interfaces, Institute of Physical Chemistry, Swiss Federal Institute of Technology, CH-1015 Lausanne, Switzerland

Received 14 March 2001; received in revised form 3 July 2001; accepted 24 July 2001

Abstract

A new series of panchromatic ruthenium(II) sensitizers derived from carboxylated terpyridyl complexes of tris-thiocyanato Ru(II) have been developed. The linkage isomers $\{(C_4H_9)_4N\}_3[Ru(Htcterpy)(–NCS)_3]$ **1**, $\{(C_4H_9)_4N\}_3[Ru(Htcterpy)(–NCS)_2(–SCN)]$ **2** and $\{(C_4H_9)_4N\}_3[[Ru(Htcterpy)(–SCN)_3]$ **3** have been separated by pH titration method and fully characterized by UV–Vis, emission, IR and NMR studies. The absorption and emission maxima of the isomer **1** show a bathochromic shift with decreasing pH, and exhibit pH-dependent excited state lifetimes. The red-shift of the emission maxima is due to better π-acceptor properties of the acid form that lowers the energy of the CT excited state. The isomer **1**, when anchored to nanocrystalline TiO_2 films achieves very efficient sensitization over the whole visible range extending into the near IR region up to 920 nm, yielding over 80% incident photon-to-current conversion efficiencies (IPCEs). Solar cells containing the isomer **1** were subjected to analysis by a photovoltaic calibration laboratory (NREL, USA) to determine their solar to electric conversion efficiency under standard AM 1.5 sunlight. A short circuit photocurrent density obtained was 20.5 mA/cm^2 and the open circuit voltage was 0.72 V corresponding to an overall conversion efficiency of 10.4%.

Keywords: Linkage isomers; Sensitizers; Dye sensitized TiO_2-based solar cells; Ruthenium complexes

1. Introduction

Dye sensitized solar cell technology is an interesting and promising inexpensive alternative to the proven solid state photovoltaic cells [1]. In recent years, many groups have been focussing their attention on fundamental aspects of dye sensitized solar cell components [2–9,24–34]. Dye derivatized mesoporous titania film is one of the key components in such cells. The electrochemical, photophysical properties of the ground and the excited state of the dye play an important role for charge transfer dynamics at the semiconductor interface [10,35]. The electron injection rates have been measured in different laboratories using the *cis*-di(thiocyanato)bis(2,2′-bipyridyl-4,4′-dicarboxylate) ruthenium(II) complex (referred as N3) and were found to occur in the femtosecond time scale [11,36,37]. We and others have obtained incident photon-to-current conversion efficiencies (IPCEs) of 80–85%, using N3 as a charge transfer sensitizer [12,38]. However, the main drawback of this sensitizer is the lack of absorption in the red region of the visible spectrum.

Molecular engineering of ruthenium complexes that can act as panchromatic charge transfer sensitizers for TiO_2-based solar cells presents a challenging task as several requirements have to be fulfilled by the dye which are very difficult to achieve simultaneously. The LUMO and HOMO of the dye have to be maintained at levels where photo-induced electron transfer into the TiO_2 conduction band and regeneration of the dye by iodide can take place efficiently. Towards this goal, we have engineered at the molecular level and synthesized a ruthenium(II) black dye in which the ruthenium center is coordinated to a tricarboxyterpyridine ligand (tcterpy = 4, 4′, 4″-tricarboxy-2, 2′, 6, 2″-terpyridine) and three thiocyanate ligands. The purpose of incorporating 4,4′,4″-tricarboxy groups in the 2,2′:6,2″-terpyridine ligand is to tune the π* molecular orbital. The role of the thiocyanato ligands is to tune the metal t_{2g} orbitals of ruthenium(II) and possibly to stabilize the hole that is being generated on the metal, after having injected an electron into the conduction band. This paper reports the

* Corresponding author. Tel.: +0041-21-693-6124; fax: +0041-21-693-4111.
E-mail address: mdkhaja.nazeeruddin@epfl.ch (Md.K. Nazeeruddin).

1010-6030/01/$ – see front matter
PII: S1010-6030(01)00572-X

synthesis and separation of linkage isomers of trithiocyanato (4,4′,4″-tricarboxy-2,2′,6,2″-terpyridine)Ruthenium(II) sensitizer.

2. Experimental

2.1. Materials

The solvents (analytical grade), potassium thiocyanate, ammonium thiocyanate, tetrabutylammonium thiocyanate, tetrabutylammonium hydroxide were purchased from Fluka. Hydrated ruthenium trichloride was purchased from Johnson Matthey and used as received. Sephadex LH-20 (Pharmacia) was allowed to swell in water for a minimum of 2 h before use. The ligand 4,4′,4″-tricarboxy-2,2′,6,2″-terpyridine was available from our previous studies [13,39].

2.2. Analytical measurements

UV–Vis and fluorescence spectra were recorded in a 1 cm path length quartz cell on a Cary 5 spectrophotometer and a Spex Fluorolog 112 Spectrofluorometer, respectively. The emitted light was detected with a Hamamatsu R2658 photomultiplier operated in single photon counting mode. The emission spectra were photometrically corrected using a calibrated 200 W tungsten lamp as reference source. The solutions were prepared to give approximate concentrations of 10 μM. The emission lifetimes were measured by exciting the sample with a pulse from an active modelocked Nd YAG laser, using the frequency doubled line at 532 nm. The emission decay was followed on a Tektronix DSA 640 Digitizing Signal Analyzer, using a Hamamatsu R928 photomultiplier to convert the light signal to a voltage waveform.

Electrochemical data were obtained by cyclic-voltammetry using a three-electrode cell and a BAS100 Electrochemical Analyzer. The working electrode was a 0.07 cm^2 glassy carbon disk, the auxiliary electrode was a glassy carbon rod, the reference electrode was AgCl/Ag, saturated KCl (0.197 V vs. SHE) and the supporting electrolyte was 0.1 M tetrabutylammonium tetrafluoroborate (TBATFB).

^{1}H NMR spectra were measured with Bruker ACP-200 spectrometers at 200 MHz. ^{13}C NMR spectra were measured with a Bruker ACP-200 at 50.3 MHz. The reported chemical shifts were against TMS.

The ex situ IR spectra were measured using a Nicolet 510 FTIR spectrometer equipped with a "Golden Gate (TM)" (Graseby-Specac) single bounce diamond-ATR accessory. The IR bench was flushed with nitrogen gas and the spectra are the average of 50 accumulated scans.

2.3. Acid–base equilibria

Since the fully protonated isomer **1** is insoluble in water, 16% of ethanol was added in order to avoid precipitation. A stock solution (5×10^{-5} M) was prepared in 100 cm^3 of 5.25/1 H_2O/ethanol mixture containing 0.1 M $NaNO_3$. The initial pH of the solution was adjusted to 11 by adding 0.2 M NaOH solution (note that the aqueous pH scale may no longer be meaningful once ethanol is added. However, at the concentration employed, ethanol had only a small effect on the pH reading of the glass electrode used). The pH of the solution was lowered by the addition of 0.2 M HNO_3 solution. The UV–Vis spectrum of each solution was measured after each addition of acid, after equilibration of the solution for 5 min. The emission spectra and the lifetime data were collected without degassing the solutions at room temperature by exciting into the lowest-energy MLCT band.

2.4. Photoelectrochemical measurements

Photoelectrochemical data were measured using a 450 W xenon light source that was focused to give 1000 W/m^2, the equivalent of one sun at AM 1.5, at the surface of the test cell. The spectral output of the lamp was matched in the region of 350–750 nm with the aid of a Schott KG-5 sunlight filter so as to reduce the mismatch between the simulated and the true solar spectrum to less than 2%. The differing intensities were regulated with neutral wire mesh attenuators. The applied potential and measured cell current was measured using a Keithley Model 2400 digital source meter. The current–voltage characteristics of the cell under these conditions were determined by biasing the cell externally and measuring the generated photocurrent. This process was fully automated using Wavemetrics software [14]. A similar data acquisition system was used to control the IPCE measurement. Under full computer control, light from a 300 W Xe lamp was focused through a high throughput monochromator onto the photovoltaic cell under test. The monochromator was incremented through the visible spectrum to generate the IPCE (λ) curve as defined below

$$\text{IPCE}\,(\lambda) = 1240\left(\frac{I_{sc}}{\lambda\phi}\right)$$

where λ is the wavelength, I_{sc} the current at short circuit (mA/cm^2) and ϕ the incident radiative flux (W/m^2). This curve can be derived from the measured absorption spectrum of the adsorbed photosensitizer for comparison.

3. Synthesis

3.1. Synthesis of $\{(C_4H_9)_4N\}_2[Ru(H_2tcterpy)(NCS)_3]$

This complex was synthesized in dark under argon atmosphere by refluxing at 130°C, a solution of H_4NNCS (2 g, in 10 ml of H_2O) and the complex [Ru(trimethoxycarbonylterpy)$(Cl)_3$] [13,39] (500 mg, in 50 ml of DMF) for 4 h. Then, 20 ml of triethyl amine and 10 ml of H_2O was added and refluxed for further 24 h to hydrolyze the ester groups on the terpyridine ligand. To the reaction flask again, was

added 20 ml of triethyl amine and 10 ml of H_2O and stirred at 100°C for 3 days. The solution volume was reduced on a rotary evaporator to about 10 ml and then, was added to 70 ml of H_2O. The resulting precipitated was filtered and taken into a 100 ml flask containing 10 ml of water. The solid was dissolved by the addition of tetrabutyl ammonium hydroxide solution in the presence of tetrabutylammonium thiocyanate. The solution was filtered and the filtrate pH was lowered to 3.5. The flask was kept in a refrigerator for 15 h at −4°C and then allowed to warm to room temperature. The resulting precipitate was collected on a sintered glass crucible. Yield 800 mg. The NMR of this product show the presence of three linkage isomers in 6:3:1 ratios that were isolated at different pH conditions (see Scheme 1). Anal. Calcd for $C_{53}H_{88}N_8O_9S_3$ Ru: C, 54.01; N, 9.51; H, 7.52. Found: C, 54.66; N, 10.07; H, 7.00. ^{1}H NMR 200 MHz, (CD_3OD) δ (ppm): 1.03 (24H, t, CH_3), 1.41 (16H, m, CH_2), 1.65 (16H, m, CH_2), 3.27 (16H, t, CH_2), 8.19 (2H, dd, H5 and H5″), 8.92 (4H, s, H3, H3′, H3″ and H5′), 9.13 (2H, d, H6 and H6″).

3.2. Separation of linkage isomers

The crude complex $\{(C_4H_9)_4N\}_2[Ru(H_2tcterpy)(NCS)_3]$ (800 mg) was taken into a 100 ml flask containing 50 ml of water. To this solution, was added 600 mg of tetrabutylammonium thiocyanate and the pH was increased to 9, by the addition of 0.1 M tetrabutylammonium hydroxide solution. The solution was filtered and the filtrate pH was lowered to 5. After reaching stable pH of 5.0, the flask was kept in a refrigerator for 12 h. Then, the flask was allowed to warm to room temperature and the resulting precipitate was collected on a sintered glass crucible. Yield 480 mg. The NMR of this compound shows the presence of only isomer **1**, i.e.,

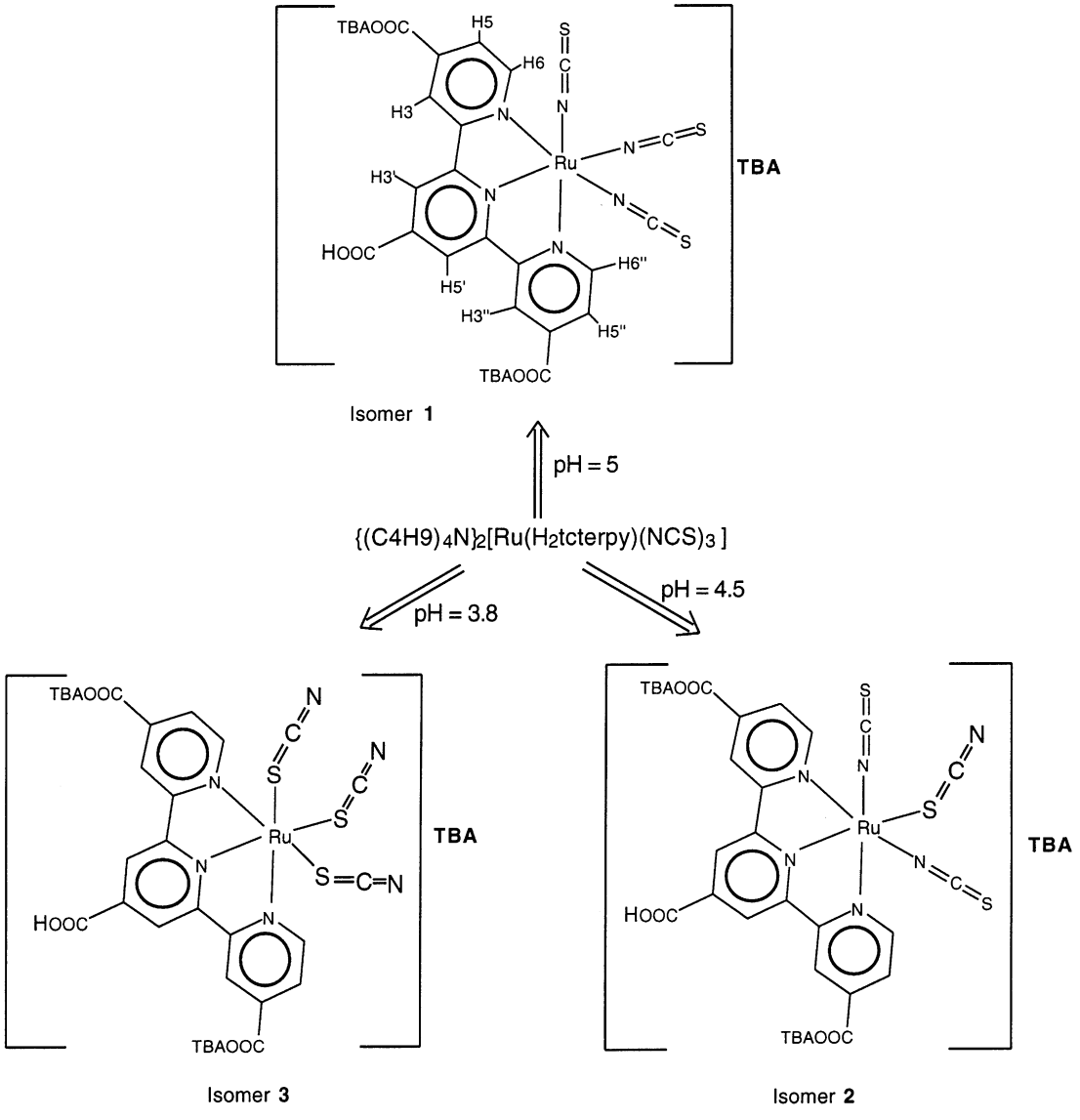

Scheme 1.

three N-bonded NCS ligands. The HPLC data show that the isolated complex is 98.5% pure.

The filtrate pH was further lowered to 4.5, and the flask was kept in a refrigerator for 12 h. The isolated product (isomer **2**) is 160 mg. The NMR of this compound shows that the product contains 80% of isomer **2** and 20% of isomer **1** that was further separated on a sephadex LH-20 column. After isolation of the isomer **2**, again the filtrate pH was lowered to 3.8, which gave isomer **3**. Yield 80 mg, and was further purified on 3 cm × 30 cm Sephadex LH-20 column, using water as an eluent.

4. Results and discussion

4.1. Separation of linkage isomers

The linkage isomers of the $\{(C_4H_9)_4N\}_2$[Ru(H_2tcterpy)$(NCS)_3$] complex were separated using a pH titration method and were further purified using a 2 cm × 30 cm, Sephadex LH-20 column using water as an eluting solvent. The difference in the pK_a values of the linkage isomers is significant, which allowed us to separate the isomers. The ruthenium metal with 4,4′,4″-tricarboxy-2,2′,6′,2″-terpyridine ligand forms a meridional configuration, in which the two peripheral pyridyl groups are *trans* to each other and electronically equivalent [15]. The central pyridine is different from the two peripheral pyridines. The ligand symmetry, which is preserved after coordination is suggestive that the pK_a of the carboxylate on the central pyridine would be different, which is *trans* to the thiocyanate, to those that are attached to the peripheral pyridines. The complex that was isolated at pH 5.0 shows the presence of only one proton that we assign to the protonation of 4′-carboxyl group of the central pyridine ring (Scheme 1). The reason for our assignment is that the central pyridine is *trans* to the more electron donating anionic NCS ligand compared to the two peripheral pyridine rings, which are less σ-donor compared to the NCS ligand. Hence, the π-back bonding to the pyridine *trans* to the NCS increases the basicity of the carboxy group resulting in a higher pK_a value compared to the remaining two pyridines [16,40].

The isomers that were isolated at pH = 4.95 and 3.8 contain all N and all S-bonded thocyanate ligands, respectively. It is interesting to note that the complex that contains S-bonded NCS ligands has a lower pK_a value than the N-bonded thiocyanate complex. The difference, in the pK_as of the isomers **1** and **3** is almost 1.2 pK_a units, which reflects the π acceptor strength of S-bonded thiocyanate ligand.

The linkage isomers of the $\{(C_4H_9)_4N\}_3$[Ru(Htcterpy)$(NCS)_3$] complex with the structural formula are given in Scheme 1. The isomer **1** that contains three N-bonded thiocyanate ligand is thoroughly characterized using by UV–Vis, emission, IR, NMR, and cyclicvoltammetric studies. The isomer **3** (Scheme 1) was characterized using UV–Vis, FTIR and NMR spectroscopy. However, the isomer **2** was not characterized fully.

4.2. FTIR spectra

FTIR spectra of the isomers were recorded in 4000–400 cm^{-1} region, as a solid using an attenuated total reflectance (ATR) spectroscopic technique. The IR spectra of the complexes containing ambidentate ligands are most informative for identifying the mode of coordination. The NCS ligands have a characteristic absorption bands depending on the N or S coordination. It has been reported that the N-coordinated NCS show ν(CN) and ν(CS) stretching vibration at 2100 and 780 cm^{-1} region [17]. Where as S-coordinated NCS show 2080 and 700 cm^{-1}.

There are five empirical methods to identify the mode of coordination based on these two stretching frequencies [18]. Epps and Marzilli [19] have isolated and characterized the linkage isomers based on the differences in the intensity of the ν(CN) band. We find that the intensity of these two stretching frequencies are more reliable compared to the other methods. The isomers **1** and **3** show a band at 2096 cm^{-1} due to ν(CN). However, the isomer **1** band is two times more intense than the isomer **3** band. The isomer **1** shows band at 788 cm^{-1} due to ν(CS). On the other hand, the isomer **3** shows band at 757 cm^{-1} due to S-bonded ν(CS) of NCS. It is interesting to note that the intensity of ν(CS) band in isomer **3** is two times higher than the ν(CS) band intensity of isomer **1** (Fig. 1).

4.3. ^1H NMR spectra

The ^{1}H NMR spectrum of isomer **1**, measured in CD_3OD solution shows three sharp and well resolved signals in the aromatic region, corresponding to the terpyridyl protons in which the two peripheral rings are magnetically equivalent. In a pseudo-octahedral geometry, a tridentate ligand like terpyridine coordinates to a metal center in a meridional fashion and the thiocyanate ligands are in an orthogonal plane. The lowest field doublet centered at δ 9.13 ppm is assigned to H6 and H6″ proton of the pyridine ring, which is *cis* to the NCS groups. The singlet at δ 8.92 ppm is due to H3, H3′, H5′ and H3″ and the doublet centered at δ 8.19 ppm assigned to the H5 and H5″ proton.

In the aliphatic region, a triplet centered at 3.27, two multiplets at 1.65 and 1.41 and a triplet at 1.03 ppm are assigned to the tetrabutylammonium cation. The integrated ratio between aliphatic protons to aromatic protons in isomer **1** shows that each ruthenium center has three tetrabutylammonium cations.

The proton NMR spectrum of the isomer **2** in deuterated methanol shows a pattern of doublet, singlet, singlet and doublet due to H6 and H6″, H3′ and H5′, H3 and H3″, H5 and H5″, respectively. The H6 and H6″ proton positions in the isomers **2** and **3**, are high field shifted compared to the isomer **1**. Another interesting difference between isomers **2**

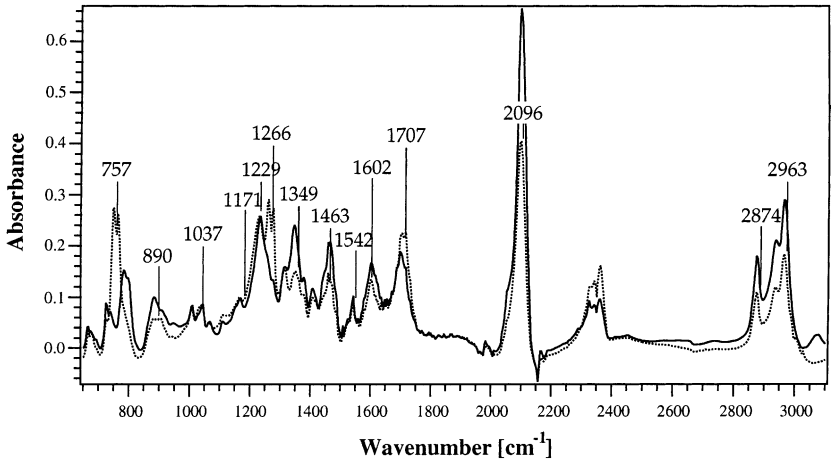

Fig. 1. Infrared absorption spectra (650–3050 cm^{-1}) of linkage isomers measured in the powder form using an ATR-IR spectrometer: solid line isomer **1** and dashed line isomer **3**.

and **3** when compared to the isomer **1** is the presence of two separate singlets in the former compared to one singlet in the later (see Table 1 and Scheme 1). The integrated ratio between the aliphatic to aromatic protons in isomers **2** and **3** show the presence of three tetrabutylammonium cations per ruthenium center.

4.4. UV–Vis absorption spectra

The UV–Vis spectra of the three isomers are dominated by metal to ligand charge transfer transitions (MLCT) in the visible region. An ethanolic solution of isomers **1–3** show lowest MLCT maxima at 620, 590 and 570 nm, respectively (Fig. 2 and Table 1). The λ maximum of the low energy MLCT band of isomer **1** is red shifted 50 nm compared to the isomer **3**. The 50 nm red shift of the longer wavelength band in going from the fully S-bonded isomer to fully N-bonded isomer, is mainly due to the stronger electron donating power of the N-bonded thiocyanate groups compared to the S-bonded thiocyanate that decreases the energy of metal dπ orbitals.

The UV–Vis, emission and lifetime data of the isomer **1** were measured over the pH range 2–11. At pH 11, the isomer **1** is the fully deprotonated anionic form and shows MLCT bands in the visible region at 570 and 390 nm, and

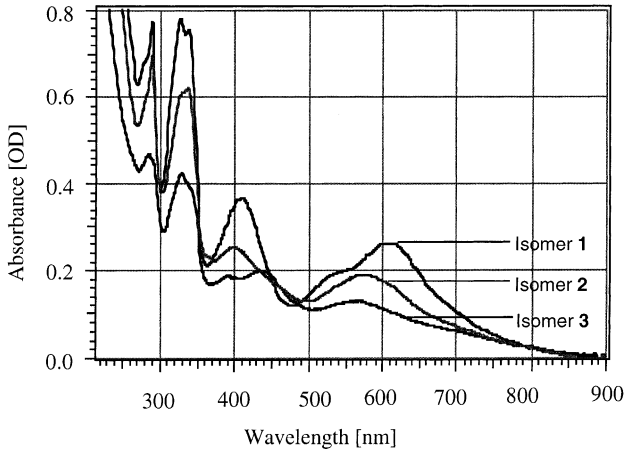

Fig. 2. Absorption spectra of the three linkage isomers.

the high energy π–π* band at 340 nm [20]. As the solution pH is lowered from 11 to 2, the MLCT transition band shifts from 570 to 600 nm with three isosbestic points at 580, 485 and 390 nm. The π–π* band shifts slightly from 340 to 345 nm. Below pH 2, precipitation under formation of a colloidal suspension of the fully protonated complex becomes apparent.

Table 1
Absorption, emission and NMR data of linkage isomers **1–3** (the emission spectra were obtained by exciting into the lowest MLCT band at room temperature)

Complex	Abs. max. (nm)[a]	Em. max. (nm)	τ (ns)[b]	^{1}H NMR[c]			
				H6, H6″	H5, H5″	H3, H3″	H3′, H5′
Isomer **1**	620	900	32	9.13 (d)	8.19 (dd)	8.92 (s)	8.92 (s)
Isomer **2**	590	820	–	9.10 (d)	8.18 (dd)	8.94 (s)	8.92 (s)
Isomer **3**	570	800	–	9.04 (d)	8.16 (dd)	8.87 (s)	8.86 (s)

[a] Measured in ethanol.
[b] Measured at room temperature.
[c] Measured in methanol-d_4.

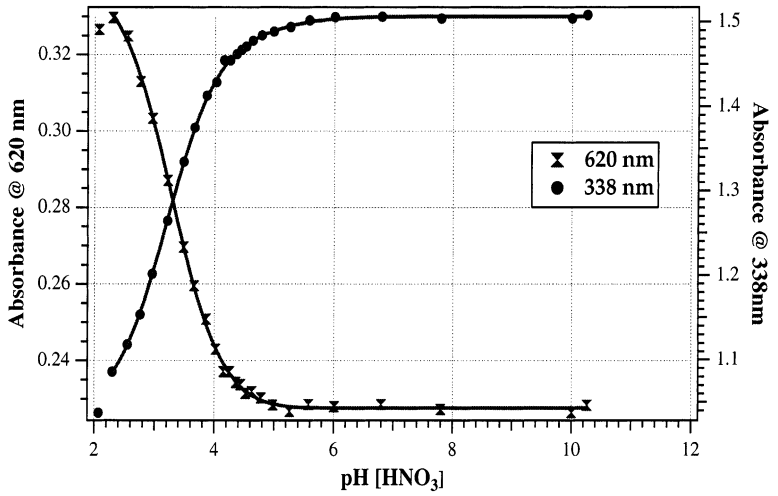

Fig. 3. Absorbance change as a function of pH for the isomer **1** at 620 and 338 nm. The solid line is calculated with the pK_a values of 3.3 and 5.0.

There are three carboxylic groups on the 4,4′,4″ positions of the terpyridine ligand. If the protonation is stepwise, three protonation equilibria can be envisioned corresponding to these three carboxy groups. On the other hand, if it is simultaneous only one equilibrium constant is expected. Fig. 3 shows the titration curve obtained by plotting the absorbance change at 620 and 338 nm vs. pH. The plot between pH 4 and 2 shows a clear inflection point at pH = 3.3 giving the ground state pK_a value of 3.3 ± 0.1. This we assign to concurrent dissociation of two protons coming from the peripheral pyridines. This value is similar to the ground state pK_as observed for ruthenium complexes of 4,4′-dicarboxy-2,2′-bipyridine ligands [10,35]. However, there is a second inflection point at pH = 5.0 ± 0.1, which we assign to the second ground state pK_{a2} coming from the central pyridine that is *trans* to the NCS ligand. The solid line in Fig. 3 exhibits good agreement with the experimental points, which was fitted assuming that the complex has two pK_a values 3.3 and 5.0 at above pH 2.2.

4.5. Emission spectra

When isomer **1** is excited within the MLCT absorption band at 298 K in an air-equilibrated ethanolic solution, it exhibits a luminescence maximum at 900 nm and a lifetime of 32 ± 1 ns. The emission spectral profile is independent of excitation wavelength and the excitation spectrum matches well with the absorption spectrum. Isomers **2** and **3** in ethanol solution show maxima at 820 and 800 nm, respectively (Table 1). The difference in the λ_{max} of isomer **1** to that of isomer **3** is due to the stabilization of HOMO in isomer **3** compared to the isomer **1**.

The emission maxima of air-equilibrated aqueous solutions (containing 15% ethanol) of the isomer **1** at pH 11 are seen at 800 nm, which red shifts to 870 nm upon decreasing the pH to 2. No significant change in the spectral profile of the emission spectra was observed in going from pH 11 to 2.11. Fig. 4 shows the titration curve obtained by plotting the change in emission intensity at 770 and 820 nm vs. pH. The effect of protonation on the luminescence and lifetime of the isomer **1** is striking. The emission intensity decreases to ≈12% of the value at pH 11 and the lifetime of the MLCT excited state decreases from 22 to <3 ns, in going from pH 11 to 2. It is well established in the literature that the charge transfer excited states can promote proton induced deactivation and thereby shorten the excited state lifetime and quantum yields [21].

4.6. Electrochemical studies

The cyclic voltammogram of complex [Ru(trimethoxycarbonylterpy)Cl_3] measured in acetonitrile containing 0.1 M tetrabutylammonium tetrafluoroborate shows a reversible wave at 0.38 V vs. Ag/AgCl, which is attributed to the $Ru^{III/II}$ redox couple [22,41]. The isomer **1** shows a quasi-reversible wave at 0.66 vs. SCE, due to the $Ru^{III/II}$ redox

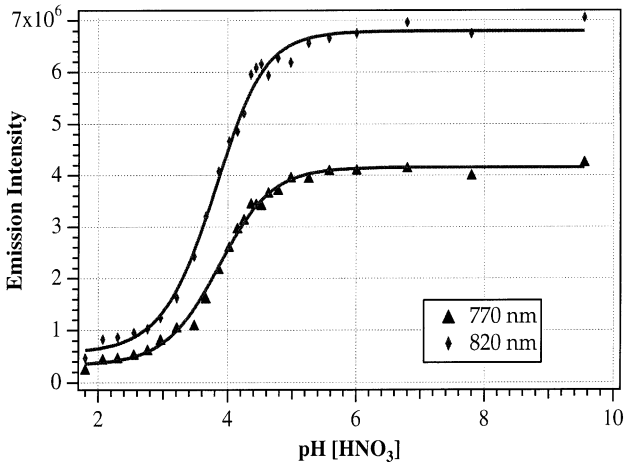

Fig. 4. Effect of pH on the emission intensity of the isomer **1** at 770 and 820 nm, in air-equilibrated aqueous solution. $\lambda_{ex} = 600$ nm.

couple. The $Ru^{III/II}$ redox potential of the thiocyanate complex (isomer **1**) is more positive than its corresponding trichloro complex and show quasi-reversible behavior. Thus, the potential for the metal-based oxidation process is shifted to a more positive value (≈0.28 V) as the chloride ligands are replaced by thiocyanate ligands, which indicate the extent of π-acceptor nature of thiocyanate ligands and is in good agreement with the parameters scale developed by Lever [23]. The oxidation peak current is higher than the reduction peak current suggesting that the thiocyanate complexes are not quantitatively being reduced in the time scale of the cyclic voltammogram. This electrochemical behavior of the thiocyanate complexes is probably due to the oxidation of the thiocyanate ligand subsequent to the oxidation of the ruthenium(II) center. In a cathodic scan, the isomer **1** display a quasi-reversible reduction wave at −1.65 V vs. Ag/AgCl, which is assigned to the terpyridine ligand-based reduction process.

4.7. Photovoltaic data

The isomer **1** solutions were prepared in ethanol (5×10^{-4} M) to which was added 20 mM of taurochenodeoxycholic acid sodium salt. The TiO_2 electrodes, which were treated with titanium tetrachloride solution were heated up to 500°C at a rate of 35°C/min under oxygen and left at this temperature for 10 min and then allowed to cool to ≈100°C. The hot electrodes were immersed into the dye solution for 20 h. The black colored films exhibited striking performance when tested in a photovoltaic cell in conjunction with a redox electrolyte. The composition of the electrolyte is 0.6 M dimethylpropylimidazolium iodide, 0.1 M of iodine, 0.5 M *tert*-butylpyridine and 0.1 M of lithium iodide in methoxyacetonitrile.

Fig. 5 shows the photocurrent action spectrum of such a cell containing isomer **1**, where the IPCE is plotted as a function of wavelength. The broad feature appears to cover the entire visible spectrum and extending into the near IR region up to 920 nm, the IPCE value in the plateau region being about 80%. Taking the light losses in the conducting glass due to optical interfaces into account the efficiency of electric current generation is practically 95% over a broad wavelength range extending from 400 to 700 nm. The overlap integral of this curve with the standard global AM 1.5 solar emission spectrum yields a short circuit photocurrent density (I_{sc}) of 20 mA/cm^2. The open circuit potential (V_{oc}) is 720 mV and the fill factor (ff) is 0.7 yielding for the overall solar (global AM 1.5 solar irradiance 1000 W/m^2) to chemical conversion efficiency a value of 10%. These results were confirmed at the National Renewable Energy Laboratory (NREL), Golden, CO.

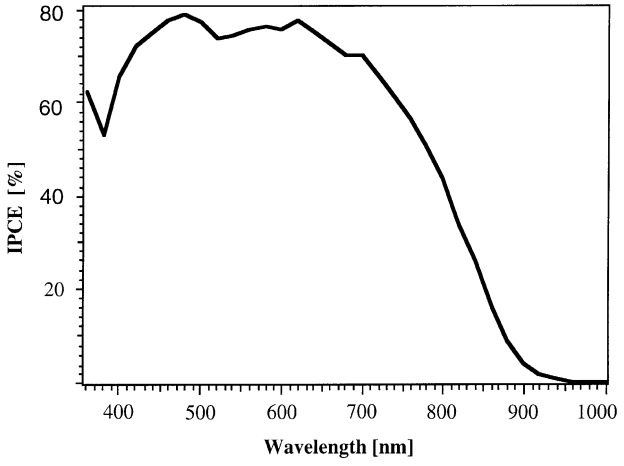

Fig. 5. Photocurrent action spectrum obtained with the isomer **1** attached to nanocrystalline TiO_2 films. The IPCE is plotted as a function of the wavelength of the exciting light.

5. Conclusions

We have succeeded in separating linkage isomers using a pH titration method. The absorption and emission maxima of the N-bonded isomer show a red shift when compared to the S-thiocyanate isomers. Based on photovoltaic performance measured under full AM 1.5 sunlight, the isomer **1** is superior to all charge transfer sensitizers known so far. The spectral response in the red and near IR region is enhanced with respect to the widely used N3 dye resulting in higher short circuit photocurrents, even though its extinction coefficient is significantly lower than the value for the latter dye.

Acknowledgements

We acknowledge financial support of this work by the Swiss Science Foundation, Swiss Federal Office for Energy (OFEN) and the Institute for Applied Photovoltaics (INAP, Gelsenkirchen, Germany). We thank Drs. R. Humphry-Baker and F.P. Rotzinger for their valuable discussions and M. Jirousek, P. Liska, L. Cevey and P. Comte for their excellent assistance with the laboratory work. We are grateful to Dr. R. Houriet, Department of Materials Science, Swiss Federal Institute of Technology, for his assistance in measuring ATR–FTIR spectra.

References

[1] R.D. McConnell (Ed.), Future Generation Photovoltaic Technologies, Proceedings of the American Institute of Physics Conference, Vol. 404, Denver, American Institute of Physics, Woodbury, New York, 1997.
[2] G. Schlichthörl, N.G. Park, A.J. Frank, J. Phys. Chem. B 103 (1999) 782.
[3] S. Ferrrere, B.A. Gregg, J. Am. Chem. Soc. 120 (1998) 843.
[4] C.A. Kelly, F. Farzad, D.W. Thompson, J.M. Stipkala, G.J. Meyer, Langmuir 15 (1999) 7047.
[5] K. Schwarzburg, F. Willig, J. Phys. Chem. B 103 (1999) 5743.

[6] A. Solbrand, A. Henningsson, S. Södergren, H. Lindström, A. Hagfeldt, S.-E. Lindquist, J. Phys. Chem. B 103 (1999) 1078.
[7] K.K. Bando, Y. Mitsuzuka, M. Sugino, H. Sughihara, K. Sayama, H. Arakawa, Chem. Lett. (1999) 853.
[8] R. Argazzi, C.A. Bignozzi, G.M. Hasselmann, G.J. Meyer, Inorg. Chem. 37 (1998) 4533.
[9] K. Tennakone, G.R.R.A. Kumara, I.R.M. Kottegoda, V.P.S. Perera, Chem. Commun. (1999) 15.
[10] Md.K. Nazeeruddin, E. Muller, R. Humphry-Baker, N. Vlachopoulos, M. Grätzel, J. Chem. Soc., Dalton Trans. (1997) 4571.
[11] J.B. Asbury, R.J. Ellingson, H.N. Ghosh, S. Ferrere, A.J. Nozik, T. Lian, J. Phys. Chem. B 103 (1999) 3110.
[12] Md.K. Nazeeruddin, A. Kay, I. Rodicio, R. Humphry-Baker, E. Muller, P. Liska, N. Vlachopoulos, M. Grätzel, J. Am. Chem. Soc. 115 (1993) 6382.
[13] Md.K. Nazeeruddin, P. Pechy, M. Grätzel, Chem. Commun. (1997) 1705.
[14] Wavemetrics. http://www.wavemetrics.com/.
[15] W.J. Perez, C.H. Lake, R.F. See, L.M. Toomey, M.R. Churchill, K.J. Takeuchi, C.P. Radano, W.J. Boyko, C.A. Bessel, J. Chem. Soc., Dalton Trans. (1999) 2281.
[16] P.A. Anderson, R.F. Anderson, M. Furue, P.C. Junk, F.R. Keene, B.T. Patterson, B.D. Yeomans, Inorg. Chem. 39 (2000) 2721.
[17] K.S. Finnie, J.R. Bartlett, J.L. Woollfrey, Langmuir 14 (1998) 2744.
[18] K. Nakamoto (Ed.), Infrared and Raman Spectra of Inorganic Coordination Compounds, 5th Edition, Wiley, New York, 1997.
[19] L.A. Epps, L.G. Marzilli, Inorg. Chem. 12 (1973) 1514.
[20] A. Mamo, A. Juris, G. Calogero, S. Campagna, Chem. Commun. (1996) 1225.
[21] N.P. Ayala, C.M. Flynn, L. Sacksteder Jr., J.N. Demas, B.A. DeGraff, J. Am. Chem. Soc. 112 (1990) 3837.
[22] A. Liobet, P. Doppelt, T.J. Meyer, Inorg. Chem. 27 (1988) 514.
[23] A.B.P. Lever, Inorg. Chem. 29 (1990) 1271.
[24] S.Y. Huang, G. Schlichthörl, A.J. Nozik, M. Grätzel, A.J. Frank, J. Phys. Chem. B 101 (1997) 2576.
[25] G. Schlichthorl, S.Y. Huang, A.J. Frank, J. Phys. Chem. B 101 (1997) 8141.
[26] B.I. Lemon, J.T. Hupp, J. Phys. Chem. B 103 (1999) 3797.
[27] B.T. Langdon, V.J. MacKenzie, D.J. Asunskis, D.F. Kelly, J. Phys. Chem. B 103 (1999) 11176.
[28] D.W. Thompson, C.A. Kelly, F. Farzad, G.J. Meyer, Langmuir 15 (1999) 650.
[29] J.S. Salafsky, W.H. Lubberhuizen, E. van Faassen, R.E.I. Schropp, J. Phys. Chem. B 102 (1998) 766.
[30] H. Sughihara, L.P. Sing, K. Sayama, H. Arakawa, Md.K. Nazeeruddin, M. Grätzel, Chem. Lett. (1998) 1005.
[31] K. Sayama, H. Sughihara, H. Arakawa, Chem. Mater. 10 (1998) 3825.
[32] K. Murakoshi, G. Kano, Y. Wada, S. Yanagida, H. Miyazaki, M. Matsumoto, S. Murasawa, J. Electroanal. Chem. 396 (1995) 27.
[33] M. Ihara, K. Tanaka, K. Sakaki, I. Honma, K. Yamada, J. Phys. Chem. B 101 (1997) 5153.
[34] B. Jing, H. Zhang, M. Zhang, Z. Lu, T. Shen, J. Mater. Chem. 8 (1998) 2055.
[35] Md.K. Nazeeruddin, S.M. Zakeeruddin, R. Humphry-Baker, M. Jirousek, P. Liska, N. Vlachopoulos, V. Shklover, C.H. Fischer, M. Grätzel, Inorg. Chem. 38 (1999) 6298.
[36] J.-E. Moser, D. Noukakis, U. Bach, Y. Tachibana, D.R. Klug, J.R. Durrant, R. Humphry-Baker, M. Grätzel, J. Phys. Chem. B 102 (1998) 3649.
[37] S.A. Haque, Y. Tachibana, D.R. Klug, J.R. Durrant, J. Phys. Chem. B 102 (1998) 1745.
[38] Y.-J. Hou, P.-H. Xie, B.-W.Z. Jing, Y. Cao, X.-R. Xiao, W.-B. Wang, Inorg. Chem. 38 (1999) 6320.
[39] Md.K. Nazeeruddin, P. Péchy, T. Renouard, S.M. Zakeeruddin, R. Humphry-Baker, P. Comte, P. Liska, L. Cevey, E. Costa, V. Shklover, L. Spiccia, G.B. Deacon, C.A. Bignozzi, M. Grätzel, J. Am. Chem. Soc. 123 (2001) 1613.
[40] A. Gerli, J. Reedijk, M.T. Lakin, A.L. Spek, Inorg. Chem. 34 (1995) 1836.
[41] G.J. Samuels, T.J. Meyer, J. Am. Chem. Soc. 103 (1981) 307.